3rd International Conference on Automation, Control, Engineering and Computer Science (ACECS'16)
Proceedings of Engineering & Technology
pp. 742-748

Coupling Quadripole Modelling for Describing Custom Discontinuities

Basma OUESLATI[#1], Taha BEN SALAH[#2], Chiraz LARBI[#3], Taoufik AGUILI[#4]

[#]*SYS'Com Laboratory, National Engineering School of Tunis ENIT*
BP. Le belvedere 1002, Tunis, TUNISIA
[1]basma.oueslati@gmail.com
[2]taha.bensalah@gmail.com
[3]chiraz.aguili@gmail.com
[4]taoufik.aguili@enit.rnu.tn

***Abstract*— This paper aims to make a rigorous evaluation of planar discontinuities using a coupling quadripole by estimating an accurate value of input impedance being based on a homographic relationship. Studied structure is short circuited microstrip line to validate the established homographic relationship. A parametric study on several characteristics is detailed to discuss their effect on quadripole evaluation.**

***Keywords*— quadripole, coupling, discontinuity, source**

I. Introduction

The modelling of the electromagnetic structures being based on integral methods [1, 2], it requires the use of a non-radiating source that will be placed in the circuit plan. The localized source is defined on a region of small dimensions (compared to the wavelength) in the very same circuit plan. Therefore, this source can be considered as a discontinuity higher order modes are generated at the transition source/circuit [3, 4]. Consequently, calculated impedance includes the contribution of evanescent modes at the transition source / circuit. It becomes necessary to quantify the contribution of higher order modes and analyze them to help obtaining more accurate results.

While input impedance (Z_e) seen by the source (S) depends on the dimensions of (S) and its nature, its worthy to notice that it is different from that seen at the circuit input. Actually, Z_e is not an accurate representation of real input impedance and a correction is necessary [5, 6 and 7].

To ensure this operation, Rautio and Harrington [8, 9 and 10] introduced a capacitor in parallel between the source and the access line. But, this modelling of discontinuity (represented by a single element) remains insufficient especially at higher frequencies. In the current study, we consider a quadripole (coupling quadripole). This is expressed by means of a homographic relationship. It has the advantage of being independent of closing dipole (load at (S2) plan). Indeed, for a specified source and an access line, the quadripole (Q_P) would be calculated only once. The change of the closing dipole and the source amplitude does not affect the quadripole (Q_p).

Besides, this relationship between the impedance Z_e, as a real value, and the reduced impedance z_2 at the circuit input, allows us to avoid the concept of characteristic impedance $Z_c = f(\omega)$ which is generally limited to low frequencies. However, elements constituting this quadripole depend on the dimensions of both source and circuit, the dielectric constants and especially frequency. This constitutes an additional calculation. But, we show in this paper that for a judicious choice of located source, one can define a frequency quasi-independent quadripole.

In this paper, we first introduce the homographic relationship characterizing the coupling quadripole. We expose thereafter the technique employed to determine the quadripole parameters. In the last paragraph, we present a parametric study on the source characteristics variation on the quadripole in order to determine the conditions necessary to maintain the same coupling quadripole independently of the source and the frequency.

II. Studied Structure

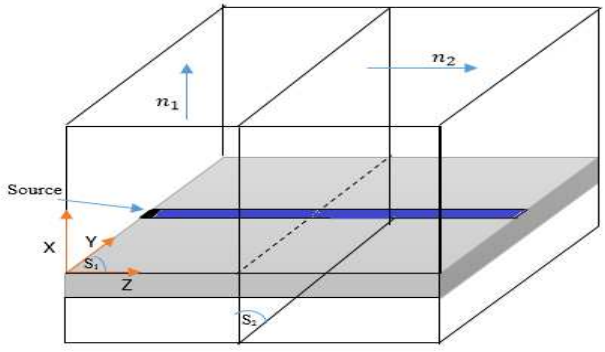

Fig. 1 Planar dipole excited by a microstrip line

Figure 1 illustrates the studied structure which is a dipole excited by a microstrip short circuited line. By introducing a current source, we can calculate the impedance seen by the source and deduce the impedance at the input of the circuit [11].

S_1 is a surface completely surrounding the source having a normal $\vec{n_1}$.

S_2 is a straight section of the microstrip line having a normal $\vec{n_2}$ oriented towards the load. It will be placed far away from the load so that the effect of higher order modes thoughtful is attenuated.

ISSN: 2356-5608

At S_1, a current density $\overrightarrow{J_1}$ is imposed, it is defined by using a unitary source $\overrightarrow{G_{01}}$ of amplitude I_1, such as:

$$\begin{cases} \overrightarrow{J_1} = I_1 \overrightarrow{G_{01}} \\ \overrightarrow{E_1} = V_1 \overrightarrow{e_1} \end{cases} \quad (1)$$

Where, $\overrightarrow{E_1}$ is the electric field in S_1

The current density $\overrightarrow{J_1}$ creates on (S_2) plan a current density and an electric field $\overrightarrow{E_2}$.

$$\begin{cases} \overrightarrow{J_2} = I_2(\overrightarrow{n_2} \Lambda \overrightarrow{h_2}) = I_2 \overrightarrow{G_{02}} \\ \overrightarrow{E_2} = V_2 \overrightarrow{e_2} \end{cases} \quad (2)$$

Where $\overrightarrow{h_2}$ and $\overrightarrow{e_2}$ represent the electromagnetic field of the unitary wave on (S_2).

With : $< \overrightarrow{G_{02}}, \overrightarrow{e_2} > = 1$

III. HOMOGRAPHIC RELATIONSHIP

At source, we determine an input impedance Z_e and at (S_2) plan, we measure an impedance z_2. This defines the proposed quadripole.

Using the concept of the impedance operator, we can write the following relations:

$$\begin{cases} \overrightarrow{E_1} = \hat{Z}_{11} \overrightarrow{J_1} + \hat{Z}_{12} \overrightarrow{J_2} \\ \overrightarrow{E_2} = \hat{Z}_{21} \overrightarrow{J_1} + \hat{Z}_{22} \overrightarrow{J_2} \end{cases} \quad (3)$$

We project the first equation of the system (3) by $\overrightarrow{J_1}$ and the second by $\overrightarrow{G_{02}}$.

$$\langle \overrightarrow{J_1} | \overrightarrow{E_1} \rangle = \langle \overrightarrow{J_1} | \hat{Z}_{11} \overrightarrow{J_1} \rangle + I_2 \langle \overrightarrow{J_1} | \hat{Z}_{12} \overrightarrow{G_{02}} \rangle \quad (4)$$

$$V_2 = \langle \overrightarrow{G_{02}} | \hat{Z}_{21} \overrightarrow{J_1} \rangle + I_2 \langle \overrightarrow{G_{02}} | \hat{Z}_{22} \overrightarrow{G_{02}} \rangle \quad (5)$$

Let: $V_2 = z_2 I_2$

We obtain:

$$I_2 = \frac{\langle \overrightarrow{G_{02}} | \hat{Z}_{21} \overrightarrow{J_1} \rangle}{z_2 - \langle \overrightarrow{G_{02}} | \hat{Z}_{22} \overrightarrow{G_{02}} \rangle} \quad (6)$$

z_2 is the input impedance seen by the line, it is expressed as a normalized value. Using the two equations (6) and (4), we get:

$$\frac{\langle \overrightarrow{J_1} | \overrightarrow{E_1} \rangle}{|I_2|^2} = \langle \overrightarrow{G_{01}} | \hat{Z}_{11} \overrightarrow{G_{01}} \rangle + \frac{\langle \overrightarrow{G_{01}} | \hat{Z}_{12} \overrightarrow{G_{02}} \rangle \langle \overrightarrow{G_{02}} | \hat{Z}_{22} \overrightarrow{G_{01}} \rangle}{z_2 - \langle \overrightarrow{G_{02}} | \hat{Z}_{22} \overrightarrow{G_{02}} \rangle} \quad (7)$$

We deduce that the input impedance Z_e seen from the source is related to the normalized input impedance z_2 seen from the line by a homographic relationship of the form (8):

$$Z_e = A + \frac{B}{C z_2 + 1} \quad (8)$$

Where A and B have the dimension of an impedance, C is dimensionless.

The homographic relationship has the great advantage to be independent of the closing dipole since the parameters of this relationship (A, B and C) are independent of the load. For a given source and a given access line, it is calculated only once. Then we can change at will the closing dipole (z_2) and the amplitude of the source.

The homographic relationship can be physically interpreted using a coupling quadripole to obtain z_2 from Z_e. Figure 2 illustrates the equivalent electrical circuit binding the input of the line to the load by a quadripole.

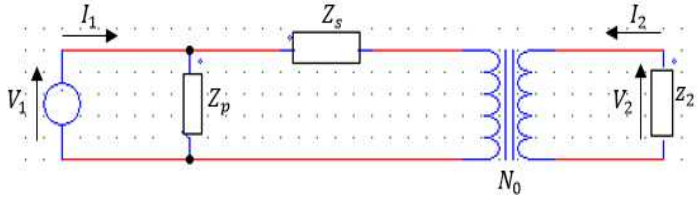

Fig. 2 The equivalent electrical circuit

This quadripole is composed of a parallel element Z_p, a serial element Z_s and a transformation ratio N_0 used to bind the input impedance Z_e in real value to the reduced impedance z_2.

Thus, we can overcome the concept of characteristic impedance Z_c which is a function of the frequency. This is interesting due to the non-uniqueness of the definition of Z_c at high frequency [12].

Using the equation (7) and the relationship between the elements of a transformer (8), we can identify Z_p, Z_s and N_0.

$$Z_e = \frac{Z_p (Z_s + z_2 / N_0^2)}{Z_p + Z_s + z_2 / N_0^2} = Z_p + \frac{-z_p^2 / (Z_p + Z_s)}{1 + z_2 / (N_0^2 (Z_p + Z_s))} \quad (9)$$

Since the homographic relationship already established is independent on the closing dipole, the determination of its parameters will be evaluated for a simple structure i.e. a microstrip short circuited line. Two approximations must be respected: first, the structure is considered as a transmission line submitted to the line's fundamental mode (characterized by its propagation constant β_g). Then, the length L (length between the short circuit and the surface S_2) should always be large enough to assume that higher order modes reflected at the level of short circuit are attenuated before reaching S_2. The expected value of the impedance seen from S_2 is given by the equation (10).

$$z_2 = jtg(\beta_g L) \quad (9)$$

With L: length between the short-circuit and the surface S_2

The coupling quadripole (or homographic relationship) consists of three unknown elements to be determined by measurements of Z_e for three line lengths L_1, L_2 and L_3. We choose e.g. the values L_1, L_2 and L_3 respectively ($3\lambda_g/2$), ($5\lambda_g/4$) and ($11\lambda_g/8$) which give at the plan (S_2) respectively z_2 value of 0, infinite and j.

Finally, this relationship obtained can be used for other studies structures and this by replacing the short circuit of closing by an open circuit or a more complex discontinuity.

IV. Determination of input impedance (seen by the source) expression (Ze)

Figure 3 illustrates the planar dipole (Figure 1) short circuited in the circuit plan.

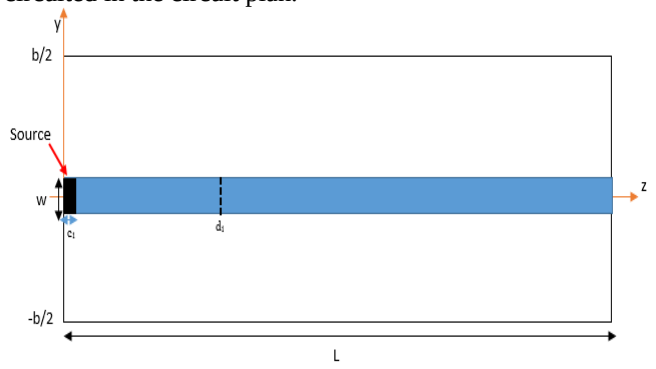

Fig. 3 Dipole short circuited: A=12.7mm, b=12.7mm, w=1.27mm, f=8GHz, c_1=0.5 mm, ε_r=10, L=49.1 mm

To determine the input impedance Z_e, we use the Galerkin method combined with Generalized Equivalent Circuit. Figure 4 illustrates the equivalent diagram of planar dipole.

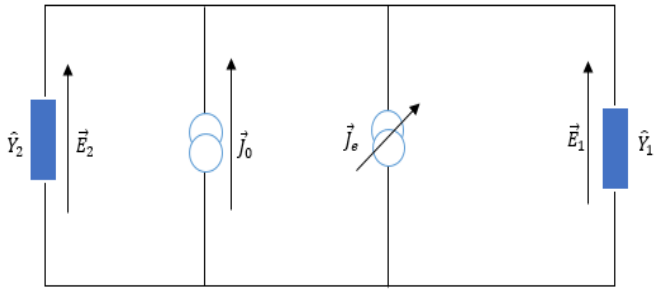

Fig. 4 Equivalent diagram of the planar dipole

$\hat{Y}_1$ and $\hat{Y}_2$ are the admittances operators defined in the basis of the TE and TM modes of the box.

$$\hat{Y} = (\hat{Y}_1 + \hat{Y}_2) = \sum_{m,n} | f_{mn} > y_{mn}^{TE,TM} < f_{mn} | \quad (10)$$

Where:

y_{mn} is the impedance of the TE and TM mode.

The impedance operator $\hat{Z}$ is given by:

$$\hat{Z} = (\hat{Y}_1 + \hat{Y}_2)^{-1} \quad (11)$$

The current source $\vec{J}_0$ defined on the source region (S) is given by:

$$\vec{J}_0 = I_0 \vec{G}_0 \quad (12)$$

The current density $\vec{J}_e$ defined on the metal (M) is given by:

$$\vec{J}_e = \sum_{i=1}^{ns} X_i \vec{G}_i \quad (13)$$

With ns is the number of test functions at convergence

The current density $\vec{J}_e$ is depicted as an adjustable source, because the amplitudes X_i of test functions $\vec{G}_i$ are calculated so as to verify the circuit boundary conditions.

$\vec{E}_0$ and $\vec{E}_M$ are the electric fields respectively defined on the source and on the metal.

$$\vec{E_0} = \hat{Z}(\vec{G_0} I_0 + \sum_{i=1}^{ns} X_i \vec{G_i}) \quad (14)$$

$$\vec{E_M} = H_M \hat{Z} (\vec{G_0} I_0 + \sum_{i=1}^{ns} X_i \vec{G_i}) = \vec{0} \quad (15)$$

The voltage source is determined as the following inner product (17):

$$V_0 = \langle \vec{G_0} | \vec{E_0} \rangle \quad (16)$$

According to equation (17), we can write:

$$V_0 = \langle \vec{G_0} | \hat{Z} \vec{G_0} > I_0 + \langle \vec{G_0} | \hat{Z} \sum_{i=1}^{ns} \vec{G_i} \rangle \begin{vmatrix} X_1 \\ \vdots \\ X_{ns} \end{vmatrix} \quad (17)$$

According to the equation (16), we can deduce the following system (19)

$$\begin{cases} \langle \vec{G_1} | \vec{E}_M \rangle = \langle \vec{G_1} | \hat{Z} \vec{G_0} \rangle I_0 + \langle \vec{G_1} | \hat{Z} \sum_{i=1}^{ns} \vec{G_i} \rangle \\ \vdots \\ \langle \vec{G_k} | \vec{E}_M \rangle = \langle \vec{G_k} | \hat{Z} \vec{G_0} \rangle I_0 + \langle \vec{G_k} | \hat{Z} \sum_{i=1}^{ns} \vec{G_i} \rangle \\ \vdots \\ \langle \vec{G_{ns}} | \vec{E}_M \rangle = \langle \vec{G_{ns}} | \hat{Z} \vec{G_0} \rangle I_0 + \langle \vec{G_{ns}} | \hat{Z} \sum_{i=1}^{ns} \vec{G_i} \rangle \end{cases} \quad (18)$$

After the resolution of the equation system (18) and (19), we have the following equation of the input impedance (20).

$$Z_e = \frac{V_0}{I_0} = z_{11} - [B]^T [A]^{-1} [B] \quad (19)$$

With:

$$A(i,j) = \langle \vec{G_i} | \hat{Z} \vec{G_j} \rangle \quad (20)$$

$$B(j) = \langle \vec{G_j} | \hat{Z} \vec{G_0} \rangle \quad (21)$$

$$z_{11} = \langle \vec{G_0} | \hat{Z} \vec{G_0} > \quad (22)$$

The test functions that we choose are of rooftop type which are most appropriate for structures having discontinuities [13, 14 and 15]. The chosen excitation source is echelon (rectangular function).

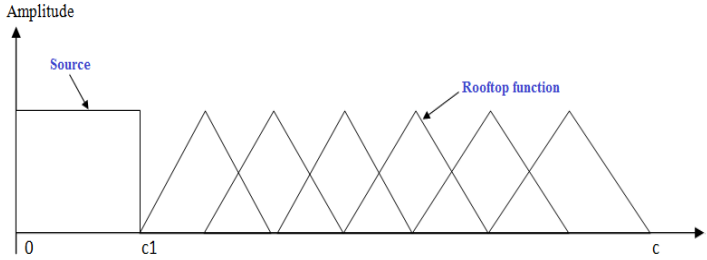

Fig 5. Echelon Source and Rooftop test functions

The source G_{01} is echelon defined as follows:

$$G_{01}(x,z)=\begin{cases}0\\ \dfrac{1}{\sqrt{w\,c_1}}\end{cases}\quad \text{for } z\in[0,c_1] \tag{23}$$

The Rooftop test functions are given by the following system (25).

$$g(x,y)=\begin{cases}N_{ATT}\dfrac{X-l+\Delta l}{\Delta l}\ for\ X\in[l-\Delta l,l]\\ -N_{ATT}\dfrac{-X+l+\Delta l}{\Delta l}\ for\ X\in[l,l+\Delta l]\\ 0\ \ Besides\end{cases} \tag{24}$$

The introduction of a planar excitation in the circuit plan allowed us to find a variational form of the input impedance. The treatment of this discontinuity problem is brought back to the study of an equivalent electrical circuit introducing a coupling quadripole. This quadripole allows us to correct the value of the input impedance (Z_e) and to have the true value of the input impedance seen by the line (z_2). From the expression of homographic relationship, we deduced that this quadripole is independent of the load we put it in the plan (S_2).

But, it would be more interesting if we establish the conditions on the source in order to maintain the same coupling quadripole [10]. We reserve the next paragraph to perform a parametric study on characteristic parameters of the source.

V. INFLUENCE OF THE ENVIRONMENT ON THE COUPLING QUADRIPOLE

In this section, we study the effect of the variation of source parameters on the coupling quadripole. This study allowed us to establish the conditions that we must respect in order for the Qp quadripole to remain unchanged regardless of the source that satisfies these conditions. A study on the effect of variation of the frequency is also performed.

The parameters of the source that we will be varied: length, position, geometric shape and position of the source.

A. *Source The effect of the source length*

Figures 6 and 7 show that the length of the source affects the quadripole elements Z_p, Z_s and N_o.

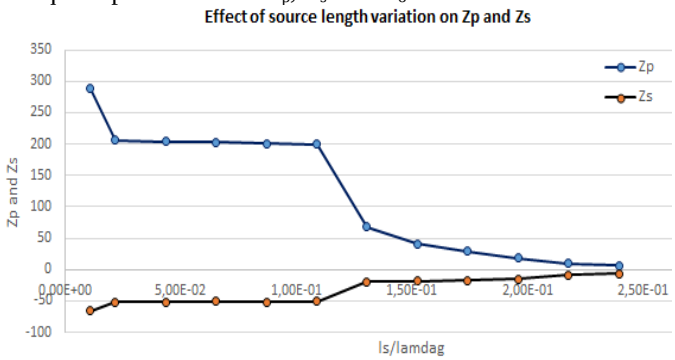

Fig 6. The effect of source length variation on the quadripole elements Zp and Zs

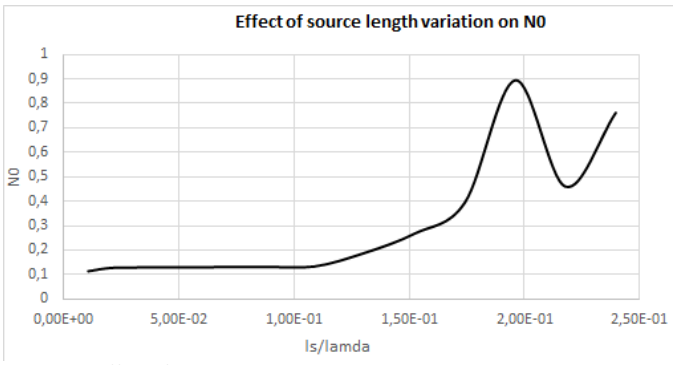

Fig 7. The effect of source length variation on No

Using the two figures 6 and 7, we can notice that the length of the source is a very important parameter which must be well chosen. For the very small lengths less than 0.02 $\lambda_g \approx \lambda_g/50$, we have a very great difference compared to other values. This can be explained by the fact that a relatively small size source tends towards a punctual source. The latter is delicate from the point of view of convergence because it requires a very high number of test functions and TE and TM modes functions. For the dimensions between 0.02 λ_g and 0.108 $\lambda_g = \lambda_g /10$, we note that we have the same values of Z_p, Z_s and N_0 with a maximum relative error of 1.955% = 2%. For source lengths greater than $\lambda_g/10$, there is a significant difference between the values found.

So to have the same coupling quadripole, the source length must be less than $\lambda_g /10$.

B. *The effect of the source function of the quadripole elements*

We have demonstrated in the previous study that when the length of the source is less than $\lambda_g /10$, we will have the same coupling quadripole. This study is done for a constant function source and a rectangular geometric shape. In this section, we will vary the source function (constant, triangular, circular and sinusoidal) and analyze its influence on our quadripole.

TABLE I
THE VALUES OF Z_P, Z_S AND N_0 AS THE FUNCTION OF THE SOURCE

Source	Zin_1	Zin_2	Zin_3	Z_p	Z_s	N_o
Triangle	-69,142	205,459	-201,643	205,459	-51,732	0,1413
Constant	-68,391	204,4624	-203,094	204,4624	-51,248	0,1405
Sinusoidal	-70,001	204,2015	-207,897	204,2015	-52,129	0,1401
Half Circle	-70,891	206,6539	-202,757	206,6539	-52,783	0,1420

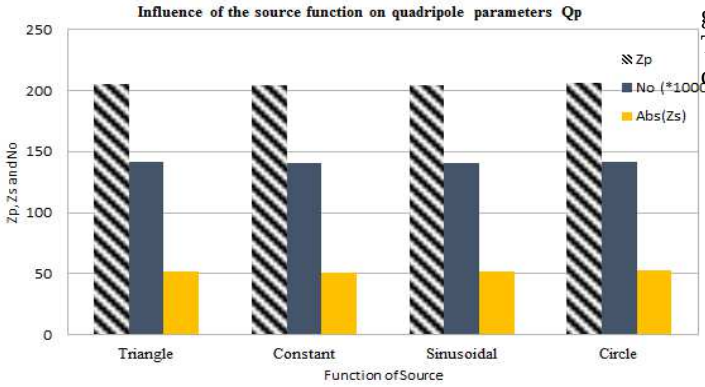

Fig 8. The effect of the choice of the source function on the quadripole elements

Figure 8 and Table 1 show that the choice of the source function does not have much influence on the coupling quadripole elements. There is a little difference, but it remains in the same order with a maximum relative error of 1.06% for Zp, 1.71% for Zs and 1.33% for No compared to the constant function. This explains the choice of constant source since it requires less test and mode functions compared to others to achieve the convergence. Table 2 show that the required number of test functions for the constant function is 6 against 13 for sinusoidal function, 11 for circular function 11 and 27 for triangular function. Similarly, the number of TE and TM mode functions is 3400 for constant, 66400 for sinusoidal , 46200 for circular and 88900 for triangular.

TABLE III
FUNCTIONS NUMBER AT CONVERGENCE

Source	Test function number	Mode function (TE and TM) number
Triangle	27	89800
Constant	6	34000
Sinusoidal	13	66400
Circle	11	46200

C. *The effect of the source geometric shape on the coupling quadripole elements*

In this section, we take a constant source of dimensions less than lambda / 10 but just by varying the geometric shape. Figure 9 illustrates the 5 geometric shapes we will be taking: triangular with two case, rectangular, half-circle and circle.

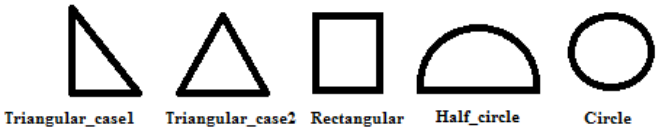

Fig 9. Different source geometric shape used

Figure 10 shows that the variation of the source geometric shape does not have a big effect on the coupling quadripole elements. The maximum error for Z_p is 1.079%, for Z_s is 5.024% and for N0 is 1.77% compared to the rectangular geometric shape. These error relative values are acceptable. The value 5% for Z_s, it is logical since it corresponds to the circular shape that is more difficult to model than others.

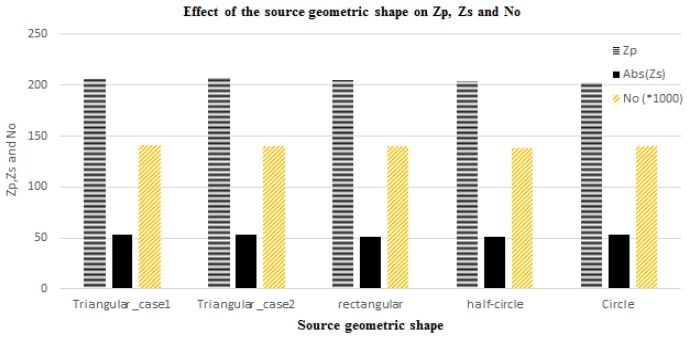

Fig 10. Effect of the geometric shape variation on Z_p, Z_s and N_0

D. *The effect of the source position on the coupling quadripole elements*

In this section, we took the case where the distance between the plan (S_2) and the plan (S_1) is $d_1 = \lambda_g$ fairly large to avoid the higher modes effect and to be able to vary the source position. From Figures 11 and 12, we observe that any position lower than 0.17 $\lambda_g \approx \lambda_g/5$, we have the same values of Z_p, Z_s and N_0. We can interpret this result by the fact that from this position begins the effect of higher modes. So, we must take into account the distance between the source and the plan (S_2) where is measured the coupling quadripole in order to avoid its effects.

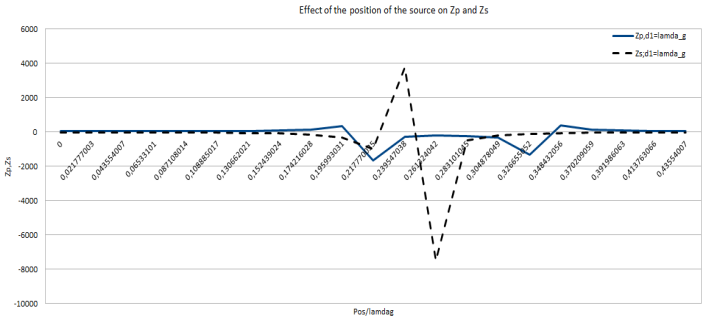

Fig 11. Effect of source position on the Zs and Zp impedances

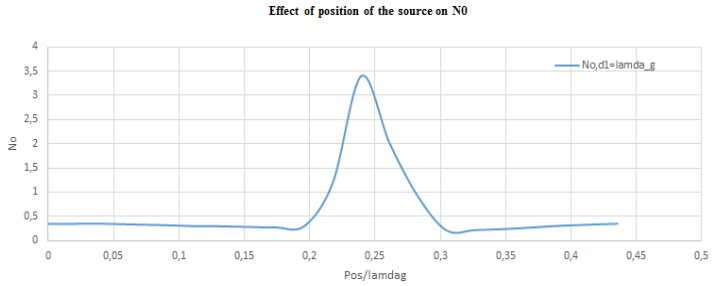

Fig 12. Effect of source position on the N_0

E. *The effect of the frequency on the quadripole elements*

In the previous study, we have focused on the source and we deduce that any source of length less than λ_g / 10 and far

away sufficiently from the plan (S_2) gives the same coupling quadripole. So, we take a constant source of rectangular geometric shape that satisfies these conditions and we vary the frequency and analyze its effect on the quadripole elements.

Figures 13 and 14 show that for frequencies lower than 9 GHz, we have the same results for Z_p, Z_s and N_0. From the frequency of 9 GHz, the behavior of these three elements is completely different. This is explained by the fact that the first higher order mode is at frequency 8.7 GHz, which makes this behavior expectable. Since we want to avoid the effect of higher order modes, we must work within a frequency range lower than 8.7 GHz.

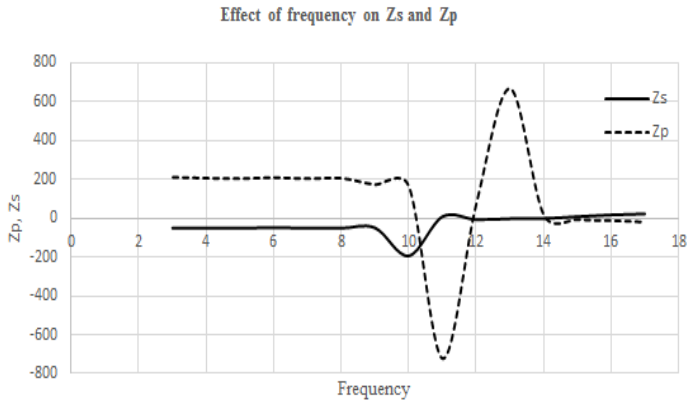

Fig 13. Effect of frequency variation on the Zs and Zp impedances

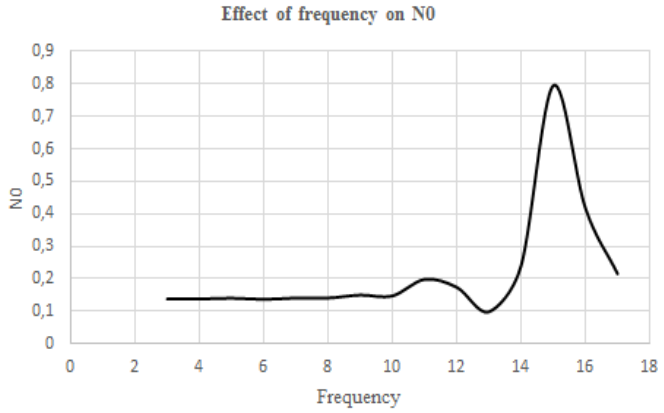

Fig 14. Effect of frequency variation on N_0

VI. Conclusion

We have introduced in this paper a quadripole to express planar discontinuity in microstrip technology. This quadripole is based on homographic relationship characterized and is characterized by three elements Z_p, Z_s and N_0. The introduction of the coupling quadripole allowed us to correct the value of the input impedance (Z_e) and to get a more accurate value of the input impedance seen by the line (Z_2) in the normalized value.

First, we have presented the study structure that is a short-circuited line having known theoretical input impedance which allows us to validate the found input impedance. Afterwards we have introduced the homographic relationship that makes finding the elements of our quadripole.

We have detailed the technique used for determining the input impedance while using Galerkin method combined with generalized equivalent circuit (MGEC).

In order for this quadripole is calculated only once, we have established a study on source parameters and also on the frequency to determine the conditions to be met.

We have deduced that any source having a length less than $\lambda_g/10$ and placed at a distance away sufficiently of the plan (S_2) and for any frequency lower than the first cutoff frequency, we have the same coupling quadripole elements with an acceptable relative errors.

References

[1] Edwards T.C. “Conception des circuits micro-ondes électroniques”, collection technologie Masson 1984

[2] Sorrentino R., « Numerical techniques for planar and quasi-planar millimeter-wave passive components », Annales des télécommunications, v 43, n 7-8, 1988, pp 392-404

[3] Worm S. B., « A full wave analysis of discontinuities in planar waveguides by the method of lines using a source approach », IEEE, Trans MTT vol 38, n10, oct 1990, pp 1510-1513

[4] El Gouzi, M. E. A. and M. Boussouis, “Hybrid method for analyse discontinuities in shielded microstrip,” International Journal of Engineering Science and Technology, Vol. 2, No. 7, 2010.

[5] Pujol S., Baudrand H., and Hanna F., “A complete description of a source type method for modelling planar structures”, Ann Telecom, 48, n 9-10, 1993, pp.459-470

[6] Koster N., Janson H., “The microstrip step discontinuity: A revised description”, IEEE, Trans, MTT, Vol 34, n 2, February 1986, pp 213-223

[7] M. A. El GOUZI, « Modélisation des discontinuités uni-axiales dans les circuits planaires par la méthode des moments », Thesis, university Abdelmalek Essaadi, June 2015

[8] J.C. Rautio and R.F. Harrington “An electromagnetic Time-Harmonic Analysis of shielded Microstrip Circuits”, IEEE Trans. Microwave Theory Tech. Vol.MTT-35, n8, pp 726-730, dec, 1987

[9] T.Aguili « Modélisation des composants S.H.F planaires par la méthode des circuits équivalents généralisés », Thesis, National Engineering School of Tunis ENIT, May 2000.

[10] T. Aguili, K.Graya, Ammar Boualègue, H.Baudrand « Application of source method for modelling step discontinuities in microstrip circuit”, IEE proceeding-Microwave, Antennas and propagation, vol. 143, n2, pp 169-173, April 1996

[11] Nadarassin M., Aubert H., Baudrand H., « Analysis of planar structrures by an integral approach using entire domain trial functions”, IEEE trans. MTT, vol 43, n10, pp 2492-2495, October 1995

[12] Knorr J.B., Tufekcioglu A.: “Spectral-domain calculation of microstrip characteristic impedance”, IEEE trans., on MTT, vol.23, n 9, September 1975, pp 725-728

[13] B.Oueslati, T. B. Salah, C.larbi, T. Aguili « A comparison between the tests functions used in the Galerkin method”, IPWIS 2013 in Tunisia

[14] Eibert T. F., Hansen V., “triangular and rectangular elements in the spectral domain stuidy of arbitrarily shaped planar circuit”, IEEE Trans., on antennas and propagation, vol. AP-41, n8, August 1993, pp.1145-1147

[15] Horng T.S., McKinzie W. E., Alexoploulos N. G., “Full-wave spectral domain analysis of compensation of microstrip discontinuities using triangular subdomain functions”, IEEE, Trans., vol. MTT-40, n12, Dec. 1992, pp.2137-2148